A VARIABLE-SIZE IFEM FOR REAL TIME SHAPE SENSING OF A LARGE HONEYCOMB ANTENNA PANEL– LATAM-SHM 2023

TIANYU DONG, SHENFANG YUAN* AND TIANXIANG HUANG *

* Research Center of Structural Health Monitoring and Prognosis
State Key Lab of Mechanics and Control for Aerospace Structures
Nanjing University of Aeronautics and Astronautics, Nanjing 210016, China
e-mail: ysf@nuaa.edu.cn

* Research Center of Structural Health Monitoring and Prognosis
State Key Lab of Mechanics and Control for Aerospace Structures
Nanjing University of Aeronautics and Astronautics, Nanjing 210016, China
e-mail: tianxiang.huang@nuaa.edu.cn

Key words: Shape sensing, large-scale structure, real-time, iFEM, variable-size element division.

Abstract. *The deformation monitoring technology can be used to track the thermal deformation of large satellite antennas in orbit to ensure the optimal performance of the satellite. The inverse finite element method (iFEM) is a popular shape-sensing reconstruction algorithm that is utilized to deduce the continuous displacement field of a structure based on measured discrete strain data. This method is based on the principle of least squares and only requires the measurement of strain, geometric dimensions, and boundary conditions to achieve accurate reconstruction. However, in the context of large-scale structural deformation reconstruction, achieving high accuracy necessitates dividing a substantial number of inverse elements, resulting in computational complexity and low efficiency. In response to the challenges mentioned above, this paper proposed a variable-size iFEM that uses variable-size element discretization to improve real-time performance. Firstly, a finite element model of a large honeycomb antenna panel was established to calculate the strain and displacement under the distributed thermal load. Subsequently, the variable-size iFEM was employed to calculate the reconstructed displacements, utilizing the FEM strain as the algorithm input and the FEM displacement as the reference displacement. The reconstructed results of the antenna panel using both variable-size and uniform-size inverse element division are compared. The results show that the proposed variable-size iFEM exhibits higher real-time performance than the conventional uniform-size iFEM when they have similar reconstruction accuracy.*

1 INTRODUCTION

Deformation monitoring of large deployable satellite antenna structures in orbit is crucial for calibrating the antennas and guaranteeing satellite performance [1]. However, the deformation of spaceborne antennas tends to vary over time, as these antennas are inevitably subjected to unevenly distributed and time-varying thermal excitation caused by the tightly arranged radio frequency payloads. Besides, periodic movement in and out of the earth's shadow region also results in drastic temperature shifts [2]. To maintain accurate radiation patterns despite changes in the antenna’s shape, the deformation sensing should be fast enough to provide the requisite response data for the radiation-pattern-correction function [3,4]. The inverse finite element method (iFEM) [5] is a promising strain-based shape sensing method that is capable of accurately acquiring the global displacement field using only discrete strain measurements, boundary constraints, and geometric dimensions, regardless of complex external loading information or material properties.

The general iFEM formulation is based on the idea of FEM and enables the entire structure to be discretized into suitable inverse elements. Several different types of inverse elements have been developed to improve the accuracy and efficiency of reconstruction. Three different types of plate/shell inverse elements have been available for modeling engineering structures, namely the iMIN3, iQS4, and iCS8 elements, which are developed based on kinematic assumptions of the first-order shear deformation theory (FSDT) [6]. Recently, the iFEM application has been extended to thick sandwich structures, based on refined zigzag theory (RZT) formulation, where inverse-plate elements iRZT3 and iRZT4 are proposed [7].

Although iFEM has been preliminarily validated in the shape sensing of beam and plate structures, there have been few studies conducted on the shape reconstruction of large-scale honeycomb structures of spaceborne antennas. Establishing a high-fidelity iFEM model for large-scale antennas requires a considerable number of inverse elements for accurate shape reconstruction which often leads to a high computational burden and significant time requirements. To strike a balance between reconstruction accuracy and reconstruction speed, the inverse element discretization is important. Existing research has mentioned two forms of meshing strategies. The first inverse element division form depends on the geometric shape of the structure, where the inverse element nodes are uniformly positioned along the geometric boundaries. This meshing strategy is suitable for structures with regular shapes and simple deformation [8]. The second inverse element division form is based on strain distribution where areas with large and rapidly changing strain amplitudes are divided into denser elements for more accurate measurements [9,10,11].

Most of the current research on the real-time performance of iFEM has focused on the reconstruction accuracy of algorithms under dynamic load conditions[12,13]. To the author's knowledge, very few of them study the reconstruction time of large-scale structures. To address the limitations of previous research, this paper proposes a variable-size iFEM, which optimizes the inverse element discretization based on structural deformation mode to achieve the real-time as well as high accuracy shape sensing of spaceborne large-scale antenna honeycomb structures. The paper discusses the implementation of the proposed method and presents the results of the performance testing and validation. In Section 2, the basic process of the variable-size iFEM is introduced. In Section 3, the reconstruction accuracy and real-time performance of uniform-size and variable-size discretization are compared, using the honeycomb structure of a spaceborne large-scale antenna as the object of analysis. Lastly, the concluding remarks are made in Section 4.

2 INTRODUCTION OF THE VARIABLE-SIZE IFEM

The variable-size iFEM uses the variable-size element discretization to improve efficiency. The variable-size element discretization is based on the structural deformation mode to arrange different densities of inverse elements in areas with different deformation levels. After the variable-size elements division is completed, the traditional iFEM procedure is carried out to calculate the reconstruction equations for each inverse element, thereby further solving the structural displacement.

As shown in Figure 1, the four-node shell element iQS4 [14,15] is analyzed in this paper. According to the definition of nodal degrees of freedom corresponding to the local coordinates (x,y,z), the node displacement column vector $\mathbf{a}^e$ can be defined in Eq. (1)：

$$\mathbf{a}^e = \left[\left(\mathbf{a}_1^e\right)^T \quad \left(\mathbf{a}_2^e\right)^T \quad \left(\mathbf{a}_3^e\right)^T \quad \left(\mathbf{a}_4^e\right)^T \right]^T \tag{1}$$

where

$$\mathbf{a}_i^e = \left[u_i \quad v_i \quad w_i \quad \theta_{xi} \quad \theta_{yi} \quad \theta_{zi} \right]^{\mathrm{T}}, \ (i = 1,2,3,4) \tag{2}$$

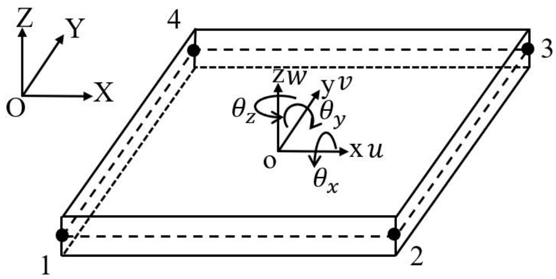

Figure 1 Four-node quadrilateral inverse-shell element iQS4

The analytical strain components of iQS4 can be expressed as:

$$\begin{aligned} \mathbf{e}\left(x, y, \mathbf{a}^{\mathrm{e}}\right) &= \mathbf{B}_{\mathbf{m}}\left(\mathbf{x}, \mathbf{y}\right)\mathbf{a}^{\mathrm{e}} \\ \boldsymbol{\kappa}\left(x, y, \mathbf{a}^{\mathrm{e}}\right) &= \mathbf{B}_{\mathbf{k}}\left(\mathbf{x}, \mathbf{y}\right)\mathbf{a}^{\mathrm{e}} \\ \mathbf{g}\left(x, y, \mathbf{a}^{\mathrm{e}}\right) &= \mathbf{B}_{\mathbf{s}}\left(\mathbf{x}, \mathbf{y}\right)\mathbf{a}^{\mathrm{e}} \end{aligned} \tag{3}$$

where $\mathbf{B}_{\mathbf{m}}(\mathbf{x},\mathbf{y})$, $\mathbf{B}_{\mathbf{k}}(\mathbf{x},\mathbf{y})$ and $\mathbf{B}_{\mathbf{s}}(\mathbf{x},\mathbf{y})$ are strain matrices used to represent the relationship between element node displacement and element strain field. The measured in-plane strains $\mathbf{e}^{\varepsilon}$ and measured curvatures $\mathbf{k}^{\varepsilon}$ can be derived from the measured surface strains on the top and bottom surfaces. The error functional of the i-th inverse finite element is defined as:

$$\phi(\mathbf{a}^{\mathrm{e}}) = \left\|\mathbf{e}(\mathbf{a}^{\mathrm{e}}) - \mathbf{e}^{\varepsilon}\right\|^2 + (2h)^2 \left\|\mathbf{k}(\mathbf{a}^{\mathrm{e}}) - \mathbf{k}^{\varepsilon}\right\|^2 + 10^{-4} \left\|\mathbf{g}(\mathbf{a}^{\mathrm{e}})\right\|^2 . \tag{4}$$

The optimization process is to make the first derivative of the error functional $\phi(\mathbf{a}^{\mathrm{e}})$ to zero and the strain-displacement relationships within the i-th inverse element discretization area can be obtained as :

$$\mathbf{k}^e\mathbf{a}^e = \mathbf{f}^e \tag{5}$$

After coordinate transformation and element assembly of the local reconstruction equations of all inverse elements shown in Eq.(5), the global reconstruction equations can be described as:

$$\mathbf{KU} = \mathbf{F} \tag{6}$$

By imposing problem-specific boundary conditions, the displacement field can be solved.

3 NUMERICAL VALIDATION

3.1 FEM model

The large-scale antenna panel as shown in Figure 2 is a honeycomb sandwich structure, and has a length width and thickness of 3125mm, 1500mm, and 20mm. A high-fidelity direct Finite Element Method (FEM) model was established to calculate the reference displacements and input strains for the iFEM application, implemented with the commercial FEM code Abaqus. T-shaped aluminum alloy blocks are considered pinned boundary conditions. The temperature of the heating and non-heating surfaces is set to 60 ℃ and 20 ℃, respectively. This paper mainly focuses on the deflection of the antenna panel.

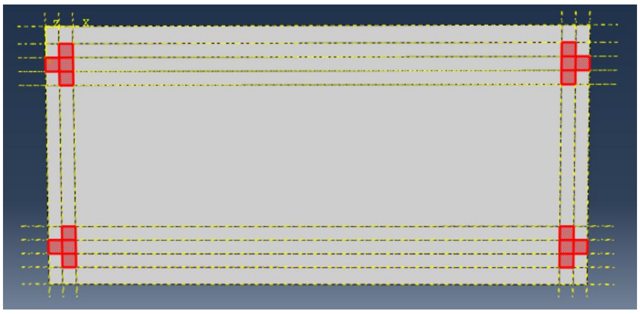

Figure 2 The FEM model of a large-scale antenna panel

3.2 Numerical results

The FEM displacement along the Z-axis of the antenna panel is shown in Figure 3 and the deformation in the middle area of the antenna panel is gentle, and the deformation near the edge is significant. Therefore, the inverse element division according to the deformation mode of the antenna panel is shown in Figure 4, in which the size of the inverse element is variable and the number of the inverse elements is 216. In order to verify the real-time performance of the proposed method in this article, a uniform-size inverse element discretization was also set up, as shown in Figure 5 with the number of inverse elements is 544.

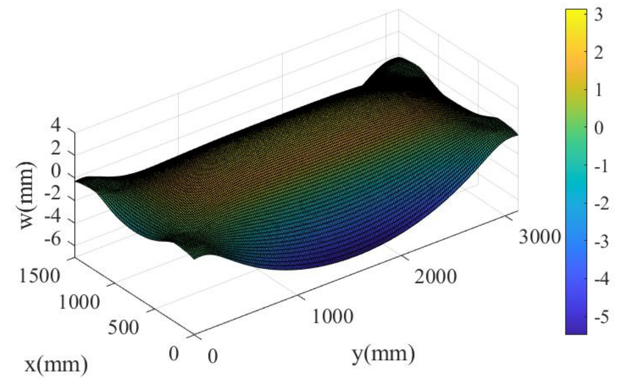

Figure 3 FEM displacement

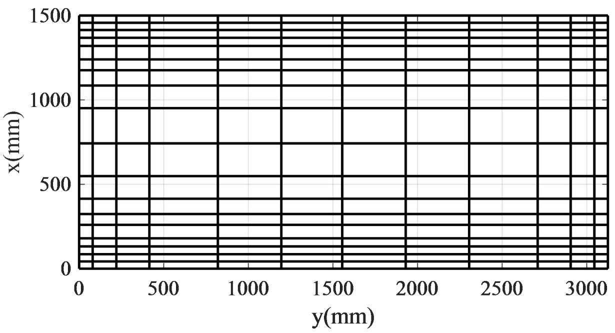

Figure 4 Variable-size inverse element discretization

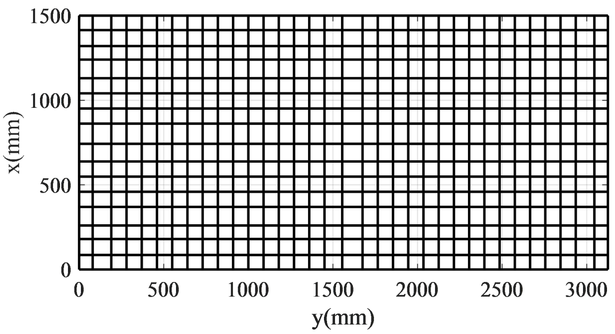

Figure 5 Uniform-size inverse element discretization

The reconstruction displacements along the Z-axis direction of the variable-size iFEM and the traditional uniform-size iFEM are shown in Figure 6. It can be seen that the variable-size and uniform-size element divisions can both accurately reconstruct the thermal deformation of the antenna panel, but the variable-size iFEM requires fewer inverse elements.

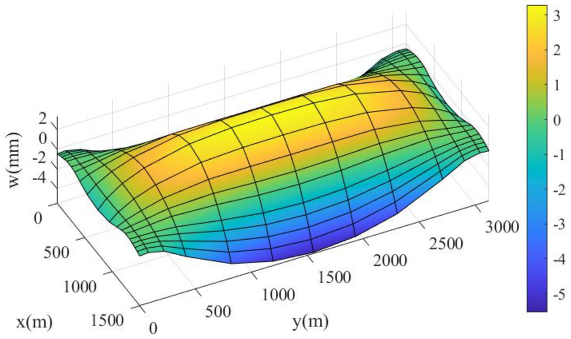

(a) variable-size element division

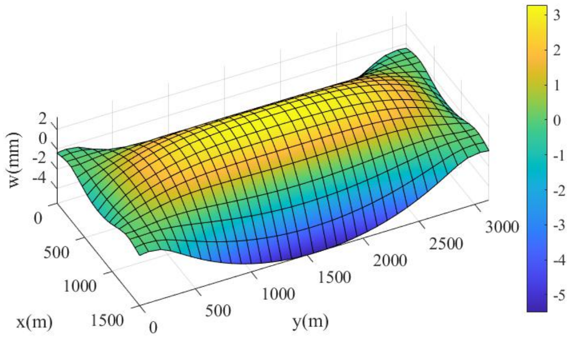

(b) uniform-size element division

Figure6 Reconstruction displacements

3.3 Results discussion

To evaluate the reconstruction accuracy, the maximum relative error were computed in relation to the direct FEM results, defined as:

$$\%e_{\max} = 100 \times \frac{\left|\mathbf{w}^{\mathbf{iFEM}} - \mathbf{w}^{\mathbf{FEM}}\right|_{\max}}{w_{\max}^{FEM}} \tag{7}$$

where $\mathbf{w}^{\mathbf{iFEM}}$ is the matrix of nodal transverse deflection of inverse analysis and $\mathbf{w}^{\mathbf{FEM}}$ is the matrix of nodal transverse deflection of direct analysis. The $\%e_{\max}$ and reconstruction time are shown in Table 1. The results show that the variable-size iFEM can achieve a similar reconstruction accuracy of 5% with fewer elements, thereby shortening the reconstruction time from 0.55 seconds to 0.12 seconds.

Table 1: Uniform inverse element division

	Uniform-size	Variable-size
$\%e_{\max}$	4.6	4.3
Reconstruction time (s)	0.55	0.12

4 CONCLUSIONS

- To improve reconstruction speed while maintaining a satisfactory level of reconstruction accuracy, this paper proposed a variable-size iFEM to realize the high-accuracy and real-time reconstruction of large antenna panels.

- The numerical results indicate that the variable-size iFEM can significantly reduce the number of inverse elements and improve the reconstruction speed by over 50%, with similar reconstruction accuracy. Therefore, the real-time and accuracy of the proposed method were verified.

5 ACKNOWLEDGMENTS

The authors are grateful for the support from the National Natural Science Foundation of China (Grant No.51921003, 52275153 and 52102475); Fundamental Research Funds for the Central Universities (Grant No. NI2023001 and NS2022064); and the Fund of Prospective Layout of Scientific Research for Nanjing University of Aeronautics and Astronautics

REFERENCES

[1] Zhang L, Gao Y, Liu X. Robust channel phase error calibration algorithm for multichannel high-resolution and wide-swath SAR imaging. IEEE Geoscience and Remote Sensing Letters, 2017, 14(5): 649-653.
[2] Wolfgang Pitz and David Miller, The TerraSAR-X Satellite, IEEE Trans. Geosci. Remote Sensing, 2010, 48, 615–622.
[3] Tessler A. Structural analysis methods for structural health management of future aerospace vehicles//Key Engineering Materials. Trans Tech Publications Ltd, 2007, 347: 57-66.
[4] Zhou J, Cai Z, Kang L, et al. Deformation sensing and electrical compensation of smart skin antenna structure with optimal fiber Bragg grating strain sensor placements. Composite Structures, 2019, 211: 418-432.
[5] Tessler A. A variational principle for reconstruction of elastic deformations in shear deformable plates and shells. National Aeronautics and Space Administration, Langley Research Center, 2003.
[6] Abdollahzadeh M A, Kefal A, Yildiz M. A comparative and review study on shape and stress sensing of flat/curved shell geometries using C0-continuous family of iFEM elements. Sensors, 2020, 20(14): 3808.
[7] Kefal A, Tabrizi I E, Yildiz M, et al. A smoothed iFEM approach for efficient shape-sensing applications: Numerical and experimental validation on composite structures. Mechanical Systems and Signal Processing, 2021, 152: 107486.
[8] Esposito M, Gherlone M. Composite wing box deformed-shape reconstruction based on measured strains: Optimization and comparison of existing approaches. Aerospace Science and Technology, 2020, 99: 105758.
[9] Kefal A, Oterkus E, Tessler A, et al. A quadrilateral inverse-shell element with drilling degrees of freedom for shape sensing and structural health monitoring. Engineering science and technology, an international journal, 2016, 19(3): 1299-1313.
[10] Tessler A. Structural analysis methods for structural health management of future aerospace vehicles//Key Engineering Materials. Trans Tech Publications Ltd, 2007, 347: 57-66.
[11] Kefal A, Oterkus E, Tessler A, et al. A quadrilateral inverse-shell element with drilling degrees of freedom for shape sensing and structural health monitoring. Engineering

science and technology, an international journal, 2016, 19(3): 1299-1313.

[12]Kefal A, Tabrizi I E, Tansan M, et al. An experimental implementation of inverse finite element method for real-time shape and strain sensing of composite and sandwich structures. Composite Structures, 2021, 258: 113431.

[13]Gherlone M, Cerracchio P, Mattone M, et al. An inverse element method for beam shape sensing: theoretical framework and experimental validation. Smart Materials and Structures, 2014, 23(4): 045027.

[14]Kefal A, Oterkus E, Tessler A, et al. A quadrilateral inverse-shell element with drilling degrees of freedom for shape sensing and structural health monitoring. Engineering science and technology, an international journal, 2016, 19(3): 1299-1313.

[15]Colombo L, Sbarufatti C, Giglio M. Definition of a load adaptive baseline by inverse finite element method for structural damage identification. Mechanical Systems and Signal Processing, 2019, 120: 584-607.